Microchimica Acta (2020) 187: 432
https://doi.org/10.1007/s00604-020-04377-6

ORIGINAL PAPER

Label-free and self-assembled fluorescent DNA nanopompom for determination of miRNA-21

Nandi Chen[1] · Junyu Li[1] · Xianzhen Feng[1] · Yanping Yang[2] · Li Zhu[1] · Xiaomeng Chen[1] · Xuan Liu[1] · Yang Li[1] · Cunchuan Wang[3] · Ligang Xia[1]

Received: 7 February 2020 / Accepted: 7 June 2020 / Published online: 7 July 2020

Abstract

A label-free fluorescence method based on self-assembled DNA nanopompom has been developed for miRNA-21 detection. In the presence of miRNA-21, three DNA hairpin probes with split G-quadruplex assemble the DNA nanopompom. Based on the isothermal toehold-mediated DNA strand displacement reaction, the target miRNA can be catalytically recycled and trigger three DNA hairpin probes to self-assemble the DNA nanopompom and release the G-quadruplex. The formation of the G-quadruplex increases the fluorescence emission intensity of thioflavin. For thioflavin-based miRNA-21 detection, the excitation and emission wavelengths are set to 425 nm and 490 nm, respectively. The limit of detection for miRNA-21 is 0.8 pM according to $F/F0 = 0.0031 \times C_{\text{miRNA-21}} + 1.0382$ ($R^2 = 0.9978$). This sensing system provides a low-cost, effective, and convenient method for miRNA detection, which holds great potential in biochemical diagnosis and clinical practice.

Keywords DNA nanotechnology · miRNA · Label-free detection · Self-assemble · G-quadruplex

Introduction

The highly specific Watson–Crick pairing of DNA molecules makes them act as both genetic information carriers and functional material units in building 2D and 3D DNA nanostructures [1]. In addition to excellent biocompatibility, the DNA nanostructures also showed controllability, cell permeability, and low immunogenicity [2]. Therefore, they are becoming promising materials in bioanalysis, molecular imaging, and drug delivery [3, 4]. DNA nanostructures could be constructed by "bottom-up" and "top-down" technology based on Watson–Crick base pairing. Both thermal annealing and an isothermal DNA self-assemble construction were applied to DNA nanostructures. For the point-of-care test, a simple strategy with lower cost and less equipment would be preferred in clinical related research [5–8]. Therefore, an isothermal DNA self-assembly procedure would be desirable for detecting cancer-related miRNA, with no requirement of annealing.

miRNAs are a class of short (18–24 nt) and non-coding RNA which are involved in cell proliferation, differentiation, stress resistance, and death. Therefore, aberrant miRNA expression contributes to disease formation and progression [9]. Traditional methods for nucleic acid detection are also used for miRNA detection, including PCR, Northern blot, and microarrays [8]. Unlike the typical analysis of gene expression, miRNAs have the characters including low abundance, short length, and sequence homology. These characters become obstacles for miRNA detection, which lead to low sensitivity,

Nandi Chen, Junyu Li and Xianzhen Feng contributed equally to this work.

Electronic supplementary material The online version of this article (https://doi.org/10.1007/s00604-020-04377-6) contains supplementary material, which is available to authorized users.

✉ Cunchuan Wang
twcc@jnu.edu.cn

✉ Ligang Xia
ligangxiaszph@hotmail.com

[1] Department of Gastrointestinal Surgery, The Second Clinical Medicine College (Shenzhen People's Hospital) of Jinan University, Shenzhen 518020, Guangdong, China

[2] Molecular Imaging Innovations Institute (MI3), Department of Radiology, Weill Cornell Medicine, 413 East 69th Street, New York, NY 10065, USA

[3] Department of General Surgery, the First Affiliated Hospital of Jinan University, No. 613 Huangpu Road, West, Guangzhou, People's Republic of China

low selectivity, and especially labor-intensive steps. Nowadays, to overcome these disadvantages, sequence-based amplification, enzyme-based assays, and nanomaterial-based sensors are also employed for miRNA detection [10–12]. To some extent, the challenges of miRNA detection have been solved.

Hybridization chain reaction (HCR) is one of the widely used methods for the isothermal DNA self-assembling, which two metastable hairpin probes self-assemble into a long polymer from an initiator sequence [13, 14]. However, for miRNA detection, HCR still has some disadvantages: (1) a typical HCR system shows a linear growth in response to the target, which might limit its signal amplification ability; (2) the target miRNA could not be cycled. It binds to the long DNA polymer after triggering the HCR. In recent years, nonlinear HCR systems have been established to achieve quadratic or exponential growth kinetics for facilitating the construction of amplified biosensing platforms [15–18]. Moreover, inspired by the enzyme-based strategy [19–21] and the catalytic hairpin assembly (CHA) [22–24], cycling the construction procedures could offer a method for increasing the sensitivity of biosensing platforms [25, 26].

Herein, we designed a target miRNA to trigger cascade and catalyzing self-assembly DNA nanopompom with three DNA hairpin probes, inspired by the isothermal DNA reaction technique included HCR, CHA, and the toehold strand displacement reaction (TSDR). This cascade assembled DNA nanostructure and repeatedly catalyzed target miRNA; then, an ultrahigh sensitivity and excellent selectivity might be achieved. In order to achieve a label-free and low-cost strategy, a split G-quadruplex was incorporated into the metastable hairpin probes. G-quadruplex structures were formed with guanine rich nucleic acid sequences, which usually induced by K+/Na+ or certain small molecules [27]. The G-quadruplex formation was triggered by the target miRNA after hairpin probe self-assembling. Thioflavin (ThT) was employed for achieving the fluorescent signal. It exhibited greater fluorescence intensity after binding to the DNA G-quadruplex structure [28]. With this characteristic, ThT is a label-free probe for fluorescent sensors; this method is simple, sensitive, and low-cost [29–32]. Our strategy allowed us to trace the miRNA-21 from colon cancer cells (HCT116) in a label-free and non-enzyme way.

Experimental

Materials and reagents

Tris (hydroxymethyl)aminomethane (Tris), acetic acid, ethylenediaminetetraacetic acid (EDTA), potassium chloride (KCl), and magnesium acetate were purchased from Sinopharm Chemical Reagent Co., Ltd. (Shanghai, China). Thioflavin (ThT) was purchased from Aladdin (Shanghai, China). Native-PAGE preparation kit and diethyl pyrocarbonate (DEPC) were purchased from Sangon Biotechnology Co., Ltd. (Shanghai, China). 2× SYBR Green qPCR Master Mix was purchased from Bimake Co., Ltd. (Shanghai, China). TransScript RT reagent Kit was purchased from TransGen Biotech Co., Ltd. (Beijing, China). All DNA and RNA sequences were purchased from General Biosystems Co., Ltd. (Anhui, China) and shown in Table S1. All solution was prepared with Milli-Q ultrapure water.

Apparatus

The fluorescent spectra were acquired with the Tecan Infinite Spark 10 M microplate reader. The excitation wavelength was set at 425 nm, and the emission spectra were collected from 440 to 580 nm (step 5 nm). Electrophoresis was processed in TBE buffer at a 20-mA constant electric current for 60 min. Gel electrophoresis was performed on the Bio-Rad Mini-PROTEAN® gel electrophoresis system and imaged on Azure Sapphire Biomolecular Imager. Dynamic light scattering (DLS) measurement was performed on a Zetasizer 3000Hs (Malvern, UK). The qRT-PCR was performed on a Bio-Rad CFX Real-Time PCR System.

Self-assembly of DNA nanostructures for miRNA-21 detection

All nucleic acid probes were centrifuged before dissolution. Hairpin probes (H1, H2, and H3) were dissolved in reaction buffer (40 mM Tris, 20 mM acetic acid, 5 mM KCl, 2 mM EDTA, and 12.5 mM magnesium acetate, pH 8.0) as 100 μM and annealed before experiments to form stable structures. ThT was dissolved in DMSO at 10 mM at first and then diluted to 100 μM (or certain concentrations) with reaction buffer. Hairpin probes were diluted to 10 μM before using and each sample contains 5 μL H1, 5 μL H2, 5 μL H3, 5 μL ThT, a certain volume of target, and added reaction buffer up to 50 μL. Various concentrations of targets were incubated with the mixture of H1, H2, H3, and ThT in reaction buffer as the optimized conditions. The fluorescent spectra were then recorded by the Tecan Infinite Spark 10M microplate reader. For fluorescence intensity detection, the excitation wavelength was set at 425 nm and the emission wavelength was set at 490 nm.

Cell culture and total RNA extraction for qRT-PCR

The colon cancer cell line HCT116, obtained from the Cell Bank of Type Culture Collection of Chinese Academy of Sciences (Shanghai, China), was cultured in McCoy's 5A

medium (Hyclone) supplemented with 10% fetal bovine serum (Gibico) and 100 U/mL penicillin/streptomycin at 37 °C in a 5% CO_2 incubator. The normal human colon mucosal epithelial cell line (NCM460), obtained from IN CELL (San Antonio, TX, USA), was cultured in RPMI 1640 medium (Hyclone) supplemented with 10% fetal bovine serum (Gibico) and 100 U/mL penicillin/streptomycin (Hyclone) at 37 °C in a 5% CO_2 incubator.

All applications for miRNA detection were soaked in 0.1% DEPC solution overnight and dried in the oven for sterilization. Buffers were pretreated with Millipore Water contained 0.1% DEPC. Trizol was used to extract total RNA from cell lines. Hemocytometer was used for counting cells. Total RNA was extracted from 10^6 cells and then diluted to a certain concentration for miRNA-21 detection. Add 0.5 mL Trizol to 10^6 cells to lyse the cells and pipet the lysate up and down several times. Incubate the homogenized sample for 5 min, centrifuge to remove the cell debris and then transfer the clear supernatant to a new tube. Add 0.1 mL chloroform for phase separation. After incubating for 3 min, centrifuge the sample for 15 min at 12000×*g* at 4 °C. The RNA is in an aqueous phase and then transferred to a new tube. Add 0.25 mL isopropyl alcohol and incubate for 10 min at 4 °C for precipitating the RNA. Then, centrifuge the sample for 15 min at 12000×*g* at 4 °C and discard the supernatant. Wash the RAN pellet 0.5 mL 75% ethanol, centrifuge at 7500×*g* for 5 min at 4 °C, and remove all leftover ethanol. Air-dry technician RNA pellet for 5–10 min and then dissolve it in Rnase-free water for qRT-PCR.

Results and discussion

The detection strategy and feasibility

DNA self-assembly triggered by the target miRNA was illustrated in Scheme 1. Triggered by miRNA-21, three metastable hairpin DNA (H1, H2, and H3) probes with split G-quadruplex were cascaded, catalyzed, and self-assembled, then the DNA nanopompom was formed. The hairpin probes contained a short loop and a long stem; particularly, the split G-quadruplex was blocked in the long stem for reduction of the leakage (DNA self-assemble without trigger). Without the target, part of the G-quadruplex was remodeled as double strand DNA, where the ThT could not insert into. Since the target miRNA would open the stem part of H1 at first, only half G-quadruplex was implanted in H1 to minimize the signal to background ratio (*F*/*F*0). The target miRNA could hybridize with the complementary region (green, 1&2) of H1 (step 1), meanwhile, it exposed part 3&4 (orange) for hybridizing its complementary region (orange, 3*&4*) in H2 (step 2). After that, the hairpin structure of H2 opened and exposed the part 5&6 (light blue) for hybridizing its complementary region with H3 (light blue, 5*&6*) and formed the G-

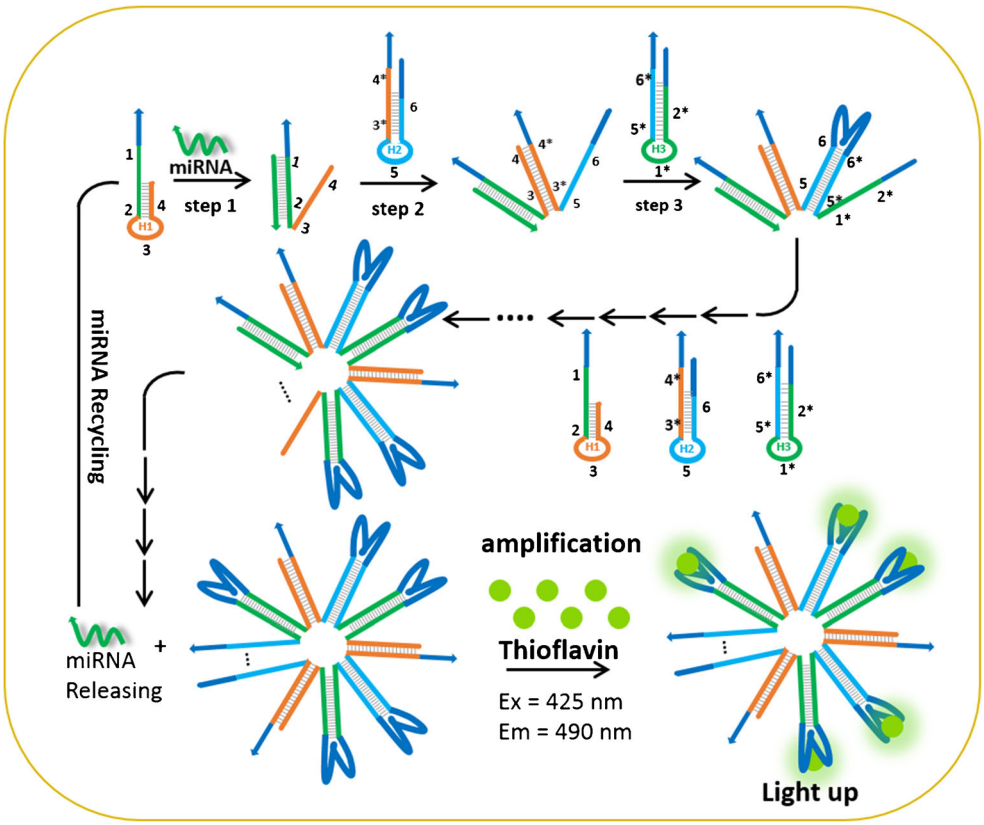

Scheme 1 Illustration of miRNA-21 triggered DNA nanopompom self-assembly

quadruplex (step 3). Meanwhile, the exposed part (green, 1*&2*) in unfolded H3 induced the cascaded DNA nanopompom self-assembly and formed more G-quadruplex. The fluorescence intensity of ThT would increase significantly when it binds to the DNA G-quadruplex. After several rounds of circulations, the DNA nanopompom would trigger the toehold strand displacement reaction and release the target miRNA for signal amplification.

Firstly, DNA nanopompom self-assembly, triggered by the miRNA-21, was characterized by Native-PAGE. As shown in Fig. 1a, when one of the hairpin probes was excluded, the DNA nanopompom could not be self-assembled (lane 2 and lane 4). In lane 3, most of the hairpin probes were observed at the lower molecular weight part on native-PAGE gel without the addition of target miRNA-21. A small leakage (self-assembly without the target miRNA-21) was also observed. With three hairpin probes and target miRNA-21 in lane 5, most of the hairpin probes self-assembled and were observed on the top of the gel, which was more than 1000 bp. The isothermally assembled DNA nanopompom was also characterized by dynamic laser scattering (DLS). In Fig. 1b, the hydrodynamic diameter was 14.34 ± 2.42 nm (PDI 0.212). These data proved the DNA nanostructures self-assembled successfully.

After PAGE verification, a ThT-based label-free fluorescence assay was set up for detecting the concentration of miRNA-21 with the self-assembled DNA nanopompom. As shown in Fig. 2, the free ThT showed relatively low fluorescence emission intensity when it was not bound to G-quadruplex (curve a). Since there was half G-quadruplex blocked in H1, the fluorescence intensity increased slightly after miRNA-21 opening the H1 (curve b). Once H2 was added, a new G-quadruplex was formed; the fluorescence intensity increased after adding H2 (curve c). In consistence with the PAGE gel characterization, minor leakage was observed in the absence of target (curve d). Most importantly, after adding the target miRNA-21 to the reaction, the ThT generated significantly amplified fluorescence emission intensity (curve d). These results suggested the feasibility of this label-free strategy for the highly sensitive detection of the target miRNA-21.

Optimization of detection conditions

To minimize the background noise and avoid the leakage (spontaneous self-assembly in the absence of target), the reaction conditions were optimized, including the concentration of ThT and K+, time, and temperature of the reaction. The signal to background ratio, $F/F0$, was used to evaluate the condition optimization results. F and $F0$ were fluorescence intensity of ThT at 485 nm in the presence and absence of target, respectively.

The stability of hairpin probes could be influenced by the temperature, then self-assembly might be triggered without target. Therefore, the incubation temperature was optimized at first by comparing with the fluorescence intensity ratio ($F/F0$). As shown in Fig. S1A, the highest ratio was obtained at 15 °C in the temperature ranging from 5 to 37 °C. A lower temperature could reduce the free energy and increase the stability of hairpin probes, resulting in the reduction of the self-assembly without target. However, once the temperature was too low, the hairpin would be hard to open and the self-assembly would be compromised. A temperature of 15 °C showed the best $F/F0$ ratio and was used for further investigation.

The incubation time could also influence the self-assembly of DNA nanopompom and the formation of the G-quadruplex, which in turn influenced the detection of target miRNA. In Fig. S1B, the $F/F0$ of various incubation time from 30 to 300 min were investigated. The $F/F0$ value increased with the increasing incubation time from 30 to 150 min and decreased slightly after that. With time extending, even no target was added, the value also increased because of the leakage.

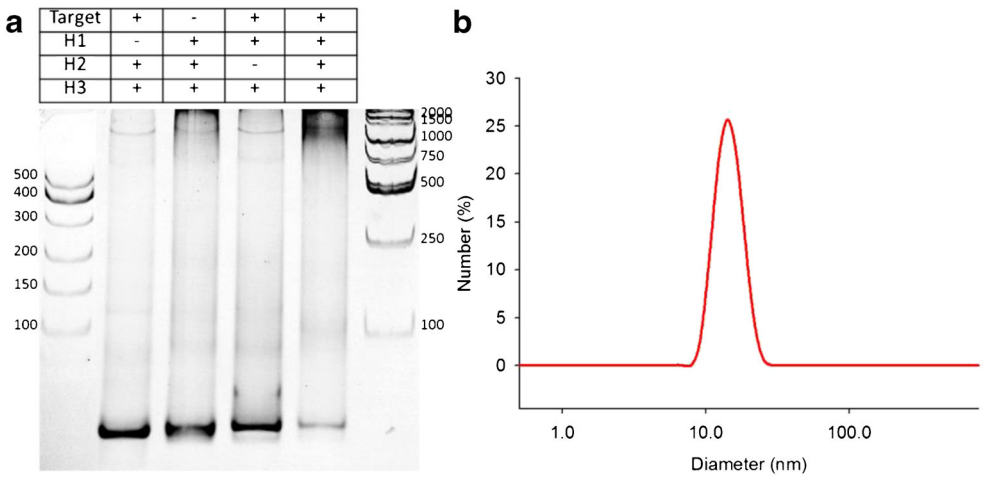

Fig. 1 **a** PAGE characterization of the miRNA-21 triggered DNA nanopompom. Target, 100 nM; H1, 3 μM; H2, 3 μM; H3, 3 μM. **b** Dynamic light scattering (DLS) showing the hydraulic diameter of the DNA nanopompom. d = 14.34 ± 2.42 nm

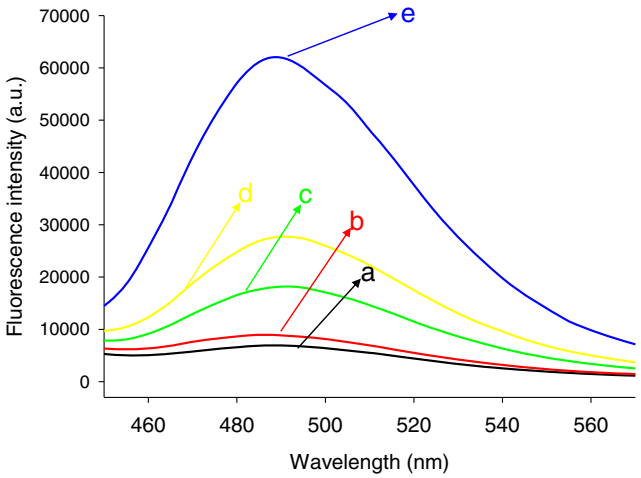

Fig. 2 Fluorescent emission spectra of miRNA-21 triggered DNA nanopompom for feasibility investigation. a: ThT, b: miRNA-21 + H1 + ThT, c: miRNA-21 + H1 + H2 + ThT, d. H1 + H2 + H3 + ThT, e: miRNA+H1 + H2 + H3 + ThT. miRNA-21, 5 nM; ThT, 5 μM; H1, 1 μM; H2, 1 μM; H3, 1 μM; incubation temperature, 20 °C; incubation time, 120 min. Ex = 425 nm, Em = 440–580 nm

Therefore, 150 min of incubation was chosen in this detection method.

Since the signal strength was based on the fluorescence emission intensity of ThT, the concentration of ThT was also a mean parameter for detecting the target miRNA. According to the value of *F*/*F*0 in Fig. S1C, the concentration of ThT did not affect the detection seriously from 2.5 to 20 μM. For achieving the highest *F*/*F*0 ratio, 10 μM ThT was chosen in this detection method.

Moreover, the concentration of K^+ ion affected the formation of the G-quadruplex and the fluorescence emission intensity of ThT. We optimized the concentration of K^+ and the result was showed in Fig. S1D. The formation of G-quadruplex was influenced by the K^+. Therefore, K^+ increased the background (without target); once there was no K^+ in the buffer, this DNA nanopompom showed the highest *F*/*F*0 ratio. Thus, no K^+ was added for selectivity and sensitivity assay.

Sensitivity and specificity

Fluorescence intensity for different concentrations of miRNA-21 was measured under the optimized condition (15 °C, 150 min, and 10 μM ThT) to demonstrate the sensitivity of this method. In Fig. 3a, the fluorescence emission intensity of ThT at 485 nm moderately increased with the increasing concentration of miRNA-21 in the range from 0 to 5000 pM. Meanwhile, as shown in Fig. 3b, the *F*/*F*0 ratio had a linear correlation once the concentration of miRNA-21 ranging from 10 to 500 pM. The regression equation was $F/F0 = 0.0031 \times C_{\text{miRNA-21}} + 1.0334$. ($R^2 = 0.9986$) The limit of detection (LOD) of miRNA-21 in our label-free detection strategy was 0.8 pM based on the mean response of the blank tests (miRNA-21 0 pM, $n = 5$) plus 3 times the standard deviation (3σ). We reviewed the label-free methods for microRNA-21 detection (Table S2). Like most label-free detection strategies, our ThT based DNA nanopompom could reduce the cost but also influenced the sensitivity. The K+ influenced the fluorescence increasing character of ThT. However, the K+ also influenced the formation of G-quadruplex and caused the leakage. After optimizing the concentration of K+ of our strategy, the highest *F*/*F*0 was achieved by with no K+ adding. A K+-insensitive fluorescence dye might be helpful for achieving a better LOD.

Besides sensitivity, we also investigated the selectivity of the miRNA-21 triggering DNA nanopompom self-assembly. Two non-target miRNAs (miRNA-199a and miRNA-141) and single- and two-base mismatched miRNA-21s were

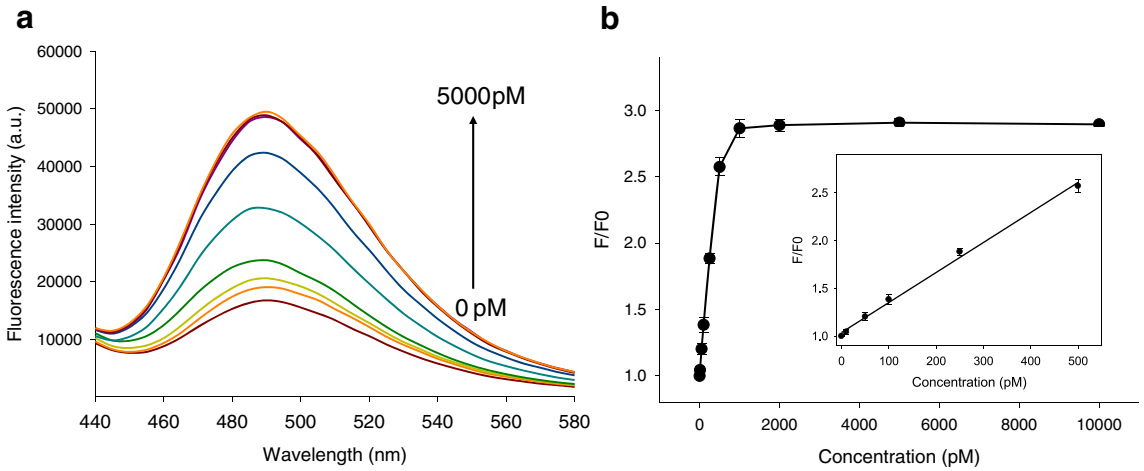

Fig. 3 **a** Fluorescence emission spectra of the ThT-based DNA nanopompom with various concentrations of miRNA-21. The concentrations of miRNA-21 are 0, 10, 50, 100, 250, 500, 1000, 2000, and 5000 pM from bottom up. Ex = 425 nm, Em = 440–580 nm. **b** Change of *F*/*F*0 with various concentrations of miRNA-21. Inset: the corresponding calibration plot of $C_{\text{miRNA-21}}$ vs. *F*/*F*0. Ex = 425 nm, Em = 490 nm, $n = 5$

chosen for selectivity assay. In Fig. 4, the concentration of the target miRNA-21 was 250 pM, while others were 10-fold excess (2.5 nM). Such a comparison indicated that only the target miRNA-21 triggered DNA hairpin self-assembly, suggesting the high selectivity of this strategy.

Applications in real samples

Cell total RNA was used as a real biological sample for investigating the practicality of this strategy. HCT116 (human colon cancer cell line) and NCM460 (human colon mucosal epithelial cell line) were chosen and results are shown in Fig. S2. HCT116 showed a more significant fluorescence intensity increase compared with NCM460 (increase from 100 cells to 50,000 cells). When there were 0 to 5000 cancer cells, the fluorescence ratio showed a linear correlation, $F/F0 = 0.002 \times C_{HCT116} + 1.0341$ ($R^2 = 0.9927$). Meanwhile, it also implied there was more miRNA-21 in HCT116 cells than NCM460 cells.

For comparison, total RNA extracted from HCT116 and NCM460 was detected by qRT-PCR together with our strategy. The concentration of miRNA-21 by qRT-PCR was calculated based on the corresponding calibration plot of $Lg_{C\ miRNA\text{-}21}$ vs the Ct value, $N_{Ct} = -3.4761 \times Lg_{C\ miRNA\text{-}21} - 9.5121$ ($R^2 = 0.9729$). The concentration of miRNA-21 by our strategy was calculated based on the corresponding calibration plot in Fig. 3b. As shown in Fig. 5, the regression equation is $C_{miRNA\text{-}21by\ qTR\text{-}PCR} = 0.9922 \times C_{miRNA\text{-}21by\ DNA\ nanopompom} + 10.877$ ($R^2 = 0.9928$, HCT116) and $C_{miRNA\text{-}21by\ qRT\text{-}PCR} = 1.1333 \times C_{miRNA\text{-}21by\ DNA\ nanopompom} + 0.6323$ ($R^2 = 0.9967$, NCM460), respectively. The DNA nanopompom–based strategy showed acceptable consistency with the commercial standard method.

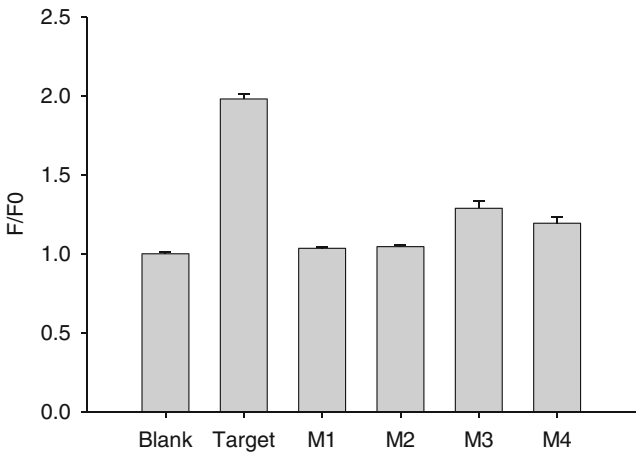

Fig. 4 Selectivity of the DNA nanopompom for miRNA-21 detection. The concentration of miRNA-21 is 250 pM, while the concentration of miRNA-199a (M1), miRNA-141 (M2), one-base mismatched (M3), and two-base mismatched (M4) miRNA is 2.5 nM. Ex = 425 nm, Em = 490 nm, $n = 5$

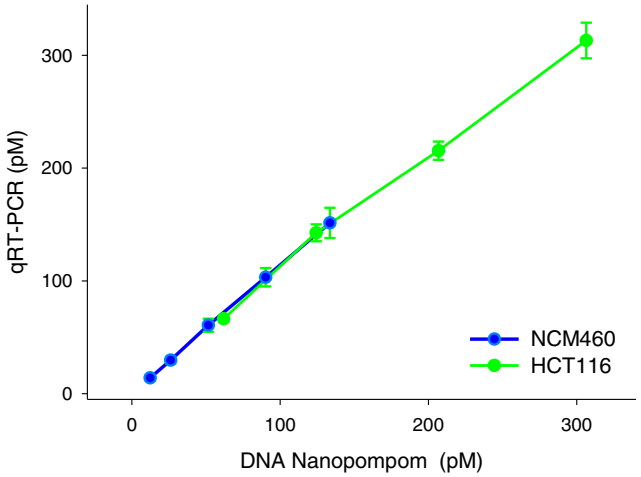

Fig. 5 The comparison between the DNA nanopompom and qRT-PCR for miRNA-21 detection in NCM460 cells (blue line) and HCT116 cells (green line). The number of NCM460 are 500, 1000, 2500, 5000, and 10,000. The number of HCT116 is 100, 250, 500, and 1000. For DNA nanopompom–based fluorescence intensity detection, Ex = 425 nm, Em = 490 nm, $n = 5$

Conclusion

Herein, a label-free DNA nanostructure was used for miRNA-21 detection. The target miRNA could be recycled catalytically for the formation of the DNA nanopompom with three hairpin DNA probes. The developing DNA nanotechnology provided powerful and convenient methods for sensitive detection of nucleic acid disease biomarkers. ThT-based strategy reduced the cost of probes but it also influenced a better LOD for its K+-sensitive character. For future work, other G-quadruplex ligands/dyes would be explored for achieving a better selectivity [29]. Moreover, imaging with a smartphone as the portable detector is also a valuable direction for the point-of-care application [33].

Acknowledgments This research was supported by the National Natural Science Foundation of China (Grant No. 81971637), the Guangdong Basic and Applied Basic Research Foundation (2019A1515110402), and the Technology & Innovation Commission of Shenzhen Municipality (Shenzhen, China; Grant No. JCYJ20190807145011340).

Compliance with ethical standards

Conflict of interest The authors declare that they have no conflict of interest.

References

1. Seeman NC, Sleiman HF (2017) DNA nanotechnology. Nat Rev Mater 3(1):1–23
2. Hu QQ, Li H, Wang LH, Gu HZ, Fan CH (2019) DNA nanotechnology-enabled drug delivery systems. Chem Rev 119(10):6459–6506

3. Xiao MS, Lai W, Man TT, Chang BB, Li L, Chandrasekaran AR, Pei H (2019) Rationally engineered nucleic acid architectures for biosensing applications. Chem Rev 119(22):11631–11717
4. Bae W, Kocabey S, Liedl T (2019) DNA nanostructures in vitro, in vivo and on membranes. Nano Today 26:98–107
5. McConnell EM, Cozma I, Morrison D, Li YF (2020) Biosensors made of synthetic functional nucleic acids toward better human health. Anal Chem 92(1):327–344
6. Ding X, Mauk MG, Yin K, Kadimisetty K, Liu CC (2019) Interfacing pathogen detection with smartphones for point-of-care applications. Anal Chem 91(1):655–672
7. Xiong Y, Zhang JJ, Yang ZL, Mou QB, Ma Y, Xiong YH, Lu Y (2020) Functional DNA regulated CRISPR-Cas12a sensors for point-of-care diagnostics of non-nucleic acid targets. J Am Chem Soc 142(1):207–213
8. Dave VP, Ngo TA, Pernestig AK, Tilevik D, Kant K, Nguyen T, Wolff A, Bang DD (2019) MicroRNA amplification and detection technologies: opportunities and challenges for point of care diagnostics. Lab Investig 99:452–469
9. Lim LP, Lau NC, Garrett-Engele P, Grimson A, Schelter JM, Castle J, Bartel DP, Linsley PS, Johnson JM (2005) Microarray analysis shows that some microRNAs downregulate large numbers of target mRNAs. Nature 433(7027):769–773
10. Masud MK, Umer M, Hossain MSA, Yamauchi Y, Nguyen NT, Shiddiky MJ (2019) Nanoarchitecture frameworks for electrochemical miRNA detection. Trends Biochem Sci 44(5):433–452
11. Goryacheva OA, Novikova AS, Drozd DD, Pidenko PS, Ponomaryeva TS, Bakal AA, Mishra PK, Beloglazova NV, Goryacheva IY (2019) Water-dispersed luminescent quantum dots for miRNA detection. TrAC Trend Anal Chem 111:197–205
12. Fiammengo R (2017) Can nanotechnology improve cancer diagnosis through miRNA detection? Biomark Med 11(1):69–86
13. Bi S, Yue SZ, Zhang SS (2017) Hybridization chain reaction: a versatile molecular tool for biosensing, bioimaging, and biomedicine. Chem Soc Rev 46:4281–4298
14. Dirks RM, Pierce NA (2004) Triggered amplification by hybridization chain reaction. Proc Natl Acad Sci 101(43):15275–15278
15. Ding X, Cheng W, Li Y, Wu J, Li X, Cheng Q, Ding S (2017) An enzyme-free surface plasmon resonance biosensing strategy for detection of DNA and small molecule based on nonlinear hybridization chain reaction. Biosens Bioelectron 87:345–351
16. Xie X, Chai Y, Yuan Y, Yuan R (2018) Dual triggers induced disassembly of DNA polymer decorated silver nanoparticle for ultrasensitive electrochemical Pb2+ detection. Anal Chim Acta 1034: 56–62
17. Li Y, Huang CZ, Li YF (2019) Ultrasensitive electrochemiluminescence detection of microRNA via one-step introduction of target-triggered branched hybridization chain reaction circuit. Anal Chem 91(14):9308–9314
18. Wei J, Gong X, Wang Q, Pan M, Liu XQ, Liu J, Xia F, Wang FA (2018) Construction of an autonomously concatenated hybridization chain reaction for signal amplification and intracellular imaging. Chem Sci 9:52–61
19. Li XT, Huang N, Zhang LL, Zhao JJ, Zhao SL (2019) A T7 exonuclease assisted dual-cycle signal amplification assay of miRNA using nanospheres-enhanced fluorescence polarization. Talanta 202:297–302
20. Hao N, Li XL, Zhang HR, Xu JJ, Chen HY (2014) A highly sensitive ratiometric electrochemiluminescent biosensor for microRNA detection based on cyclic enzyme amplification and resonance energy transfer. Chem Commun 50(94):14828–14830
21. Cui L, Zhu Z, Lin NH, Zhang HM, Guan ZC, Yang CY (2014) A T7 exonuclease-assisted cyclic enzymatic amplification method coupled with rolling circle amplification: a dual-amplification strategy for sensitive and selective microRNA detection. Chem Commun 50(13):1576–1578
22. Li BL, Ellington AD, Chen X (2011) Rational, modular adaptation of enzyme-free DNA circuits to multiple detection methods. Nucleic Acids Res 39(16):e110–e110
23. Li JB, Lei PH, Ding SJ, Zhang Y, Yang JR, Cheng Q, Yan YR (2016) An enzyme-free surface plasmon resonance biosensor for real-time detecting microRNA based on allosteric effect of mismatched catalytic hairpin assembly. Biosens Bioelectron 77:435–441
24. Jiang Y, Li BL, Milligan JN, Bhadra S, Ellington AD (2013) Real-time detection of isothermal amplification reactions with thermostable catalytic hairpin assembly. J Am Chem Soc 135(20):7430–7433
25. Zhou WJ, Liang WB, Li X, Chai YQ, Yuan R, Xiang Y (2015) MicroRNA-triggered, cascaded and catalytic self-assembly of functional "DNAzyme ferris wheel" nanostructures for highly sensitive colorimetric detection of cancer cells. Nanoscale 7(19):9055–9061
26. Zhou WJ, Li DX, Chai YQ, Yuan R, Xiang Y (2015) RNA responsive and catalytic self-assembly of DNA nanostructures for highly sensitive fluorescence detection of microRNA from cancer cells. Chem Commun 51(92):16494–16497
27. Burge S, Parkinson GN, Hazel P, Todd AK, Neidle S (2006) Quadruplex DNA: sequence, topology and structure. Nucleic Acids Res 34(19):5402–5415
28. Mohanty J, Barooah N, Dhamodharan V, Harikrishna S, Pradeepkumar PI, Bhasikuttan AC (2013) Thioflavin T as an efficient inducer and selective fluorescent sensor for the human telomeric G-quadruplex DNA. J Am Chem Soc 135(1):367–376
29. Khusbu FY, Zhou X, Chen HC, Ma CB, Wang KM (2018) Thioflavin T as a fluorescence probe for biosensing applications. TrAC Trends Anal Chem 109:1–18
30. Fan TT, Mao Y, Liu F, Zhang W, Yin JX, Jiang YY (2017) Dual signal amplification strategy for specific detection of circulating microRNAs based on Thioflavin T. Sensors Actuators B Chem 249:1–7
31. Tan XH, Wang Y, Armitage BA, Bruchez MP (2014) Label-free molecular beacons for biomolecular detection. Anal Chem 86(21): 10864–10869
32. Liu Y, Shen T, Li J, Gong H, Chen CY, Chen XM, Cai CQ (2017) Ratiometric fluorescence sensor for the microRNA determination by catalyzed hairpin assembly. ACS Sens 2(10):1430–1434
33. Sun Y, Shi L, Wang Q, Mi L, Li T (2019) Spherical nucleic acid enzyme (SNAzyme) boosted chemiluminescence miRNA imaging using a smartphone. Anal Chem 91(5):3652–3658